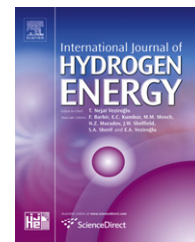


Available online at www.sciencedirect.com

SciVerse ScienceDirect

journal homepage: www.elsevier.com/locate/he

Optimization of catalyst ink composition for the preparation of a membrane electrode assembly in a proton exchange membrane fuel cell using the decal transfer

Chi-Young Jung^a, Wha-Jung Kim^b, Sung-Chul Yi^{a,c,*}

^a Department of Chemical Engineering, Hanyang University, Seoul 133-791, Republic of Korea

^b Department of Materials Chemistry and Engineering, Konkuk University, Seoul 143-701, Republic of Korea

^c Department of Hydrogen and Fuel Cell Technology, Hanyang University, Seoul 133-791, Republic of Korea

ARTICLE INFO

Article history:

Received 26 June 2012

Received in revised form

13 August 2012

Accepted 2 September 2012

Available online 1 October 2012

Keywords:

Proton exchange membrane fuel cell

Membrane electrode assembly

Decal transfer

Swelling agent

Electrochemical impedance spectroscopy

Cyclic voltammetry

ABSTRACT

For low interfacial resistance and feasibility of forming catalyst layer (CL), decal transfer (DT) is considered as one of the most effective methods for preparing a membrane electrode assembly. However, optimization of the catalyst ink composition is necessary, because of the complexity of the CL. Here, 1-propanol is adsorbed onto the CL coated onto the decal, as a swelling agent, for complete transfer of the CL onto Nafion membrane. Using this methodology, flat and complete DT is achieved at the hot-pressing conditions of 60 °C and 5 MPa. For optimization, the solvent-to-carbon ratio (SCR) and Nafion-to-carbon ratio (NCR) are controlled to achieve improved cell performance. In this study, by considering the morphology of CL and the cell performance when CL is annealed at temperatures sufficiently below the boiling point of the solvent, optimized SCR and NCR values of approximately 12.0 and 0.65, respectively, are obtained. In addition, microstructure, thickness and various electrochemical properties of the CLs are examined in detail.

Copyright © 2012, Hydrogen Energy Publications, LLC. Published by Elsevier Ltd. All rights reserved.

1. Introduction

Proton exchange membrane fuel cells (PEMFCs) are considered as one of the most promising alternatives to conventional fossil-fueled power sources. PEMFCs are very clean and efficient power sources that directly convert chemical energy of hydrogen fuel into electrical energy. Their low-temperature operating conditions make them applicable for use in the power sources of automobile and portable systems. However, breakthrough technologies are still required to achieve commercialization of PEMFCs, especially reduction in

manufacturing cost [1]. Platinum supported on carbon black (Pt/C) catalysts, which are most generally used in PEMFCs, have gradually become expensive (approximately \$54.66 per gram at present) [2], and their utilization in state-of-the-art electrodes is still low, approximately 0.28 g_{Pt} kW^{−1} [3]. As illustrated in Fig. 1, the Pt/C catalysts are aggregated with a Nafion electrolyte to form so-called flooded agglomerates with diameters ranging from 100 to 1000 nm [4,5]. In typical PEMFC catalyst layers (CLs), however, there exists a portion of the catalytic surfaces, which has poor contact with Nafion electrolyte, thus reducing platinum utilization.

* Corresponding author. Department of Chemical Engineering, Hanyang University, Seoul 133-791, Republic of Korea. Tel.: +82 2 2220 0481; fax: +82 2 2298 5147.

E-mail address: scy@hanyang.ac.kr (S.-C. Yi).

0360-3199/\$ – see front matter Copyright © 2012, Hydrogen Energy Publications, LLC. Published by Elsevier Ltd. All rights reserved.
<http://dx.doi.org/10.1016/j.ijhydene.2012.09.013>

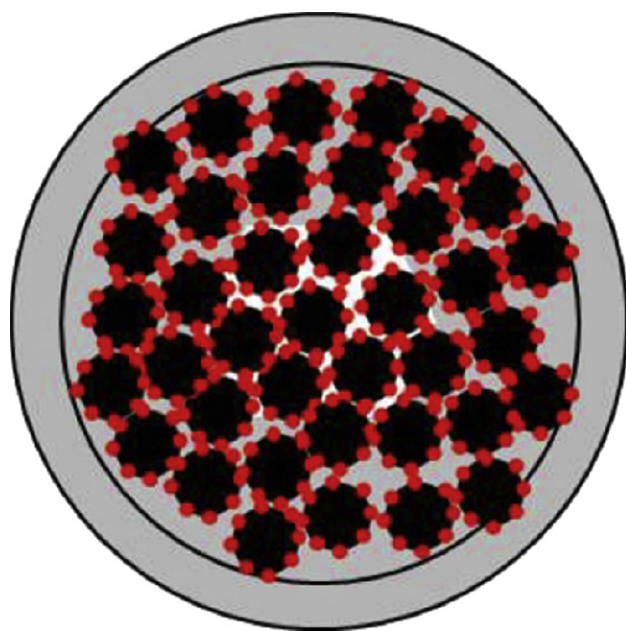


Fig. 1 – A schematic representation of the Nafion-Pt/C agglomerate: gray, black, red and white represents Nafion, carbon black, platinum and void, respectively. (For interpretation of the references to colour in this figure legend, the reader is referred to the web version of this article.)

For the last three decades, many approaches for reducing the amount of platinum loading in the CLs and increasing platinum utilization have been reported. In 1988, Ticianelli et al. [6] reported reducing platinum loading from over 1.0 mg cm^{-2} to approximately 0.4 mg cm^{-2} , without decreasing cell performance, by impregnating the catalyzed gas diffusion layer (GDL) with Nafion. In the early 1990s, Wilson et al. [7–9] reported two different methodologies for fabricating catalyst-coated-on-membrane (CCM) membrane electrode assemblies (MEAs). One method is to directly coat catalyst ink onto the membrane by spray deposition. The other is the well-known decal transfer (DT) method, which involves forming the CL on a Teflon sheet before transferring it onto the membrane by hot pressing. The CCM MEA presented similar levels of cell polarization with $0.18\text{--}0.20 \text{ mg cm}^{-2}$ of platinum loading, because better contact between CLs and membranes facilitates more efficient proton transfer than catalyst-coated-on-GDL (CCG) MEA.

Since then, numerous studies have been conducted using Wilson's DT or a modified version of DT to fabricate MEAs with low charge transfer resistance and high platinum utilization. Xie et al. [10] characterized CLs prepared by DT using mercury porosimetry. Xie et al. [11] also compared cell polarization of MEAs prepared from Teflon and Kapton decal substrates by controlling the ionomer-skin layer. Chisaka and Daiguji [12] have reported the effect of residual glycerol on cell polarization and pore distribution. Alternatively, many have focused on modified DT procedures that use low hot-pressing temperatures with protonated Nafion. These studies have all stated that typical DT might suffer incomplete transfer of CL if no modification is made. Saha et al. [13] and Cho et al. [14]

suggested that over 8 min of hot-pressing with sufficient pressure and temperature is required to achieve high transfer yield. In addition, Cho et al. [14] have claimed that incomplete transfer occasionally occurs when outer ionomer layer is not applied, regardless of whether the hot-pressing conditions are appropriate. Park et al. [15] suggested a carbon breaking layer from carbon colloidal dispersion to increase transfer yield. They provided a 100% DT yield by introducing the layer; however, the proposed procedure was more complex than typical DTs, because an additional carbon layer needed to be coated prior to the CL. Recently, Cho et al. [16] reported that liquid nitrogen treatment prior to removing the decal film assisted in achieving high transfer yield under both high and low hot-pressing temperature and pressure conditions.

Despite these efforts, optimal composition of the catalyst ink for DT is still not well understood. In general, solvents applicable for DT are limited because maintaining the printability of catalyst ink on the decal is a very complex issue, especially when different substances are used [8,9,12]. This is the main reason why most DT experiments have been conducted with isopropyl alcohol, glycerol or glycerol-like solvents [10–13], such as ethylene glycol, propylene glycol, etc. According to recent molecular-dynamics simulations [17] and voltammetric experiments [18], catalyst ink composition is crucial, because interfacial properties arising from Nafion-Pt or Nafion-carbon relation can be varied. In addition, Bender et al. [19] reported that preparing 10 MEA samples took 24 h of annealing duration when DT was applied. Therefore, optimizing catalyst ink composition, including amount of solvent and Nafion, is important to reduce the cost and improve cell performance.

The main objectives of this study are to provide optimized composition of the catalyst ink in the preparation of MEA using modified DT. By applying appropriate amount of 1-propanol as a plasticizer, a low-temperature DT is used to prepare all MEA samples. The effects of solvent-to-carbon ratio (SCR) and Nafion-to-carbon ratio (NCR) were examined by carefully controlling the composition of catalyst ink, dispersing method and decaling process. Microstructure and electrochemical properties of the electrodes were examined by cell polarization, electrochemical impedance spectroscopy (EIS) and cyclic voltammetry (CV).

2. Experimental

2.1. Preparation of the membrane electrode assembly

To prepare the MEA, a modified DT procedure [20] was used to form ultrathin CLs on the proton exchange membrane. The catalyst inks were prepared at a concentration of 5 wt.% Nafion solution (DE512, Ion Power, New Castle, DE, USA), carbon-supported platinum catalyst (HiSPEC 3000, Alfa Aesar, Ward Hill, MA, USA) and glycerol (99.5 wt.%, Sigma Aldrich, St. Louis, MO, USA). After the ink was homogeneously dispersed, tetrabutylammonium hydroxide (40 wt.%, Alfa Aesar) was added to convert H-form Nafion into TBA-form Nafion. The resulting dispersion was stirred with a magnetic bar for 24 h and dispersed in a sonication bath for 1 h to obtain a homogeneous solution.

Subsequently, the Teflon films were repeatedly painted with the ink and annealed in the convection oven at the appropriate temperature until the platinum loading reached 0.20 mg cm^{-2} . The temperature in the oven is very important, because the rate of solvent evaporation is crucial to stable formation of a CL. An annealing temperature of 135°C is used to evaporate glycerol. After the CL is formed, a sufficient amount of 1-propanol (99.5 wt.%, Sigma Aldrich) was applied to induce the plasticizer effect and obtain a high transfer rate of over 95% under low hot-pressing temperature and pressure conditions.

A Nafion membrane (NRE212, Ion Power) was selected for the proton exchange membrane. First, the Nafion membranes were converted into Na-form Nafion by lightly boiling in 1 wt.% sodium hydroxide aqueous solution, followed by boiling in deionized water. After that, the CL-coated decal was assembled by sandwiching the Na-form Nafion membrane and hot-pressing at 60°C for 10 min. After the Teflon sheet was peeled off, the MEA was soaked into boiling sulfuric acid solution and deionized water to convert it into H-form MEA. The resulting MEA was wiped and dried for over 1 h in a vacuum dryer before characterization. Fig. 2 illustrates the DT process that is used to prepare all the samples in this work.

In a typical DT process, glycerol is widely used because it is dipolar solvent with high dielectric constant and viscosity, resulting in less aggregation and excellent paintability. Therefore, evaluating the effect of SCR and NCR was conducted using glycerol. Separate studies (varying SCR at a fixed NCR, then varying NCR at a fixed SCR), rather than one factorial study co-varying both GCR and NCR were performed to exclude possible interactions between these factors. For NCRs, relatively low values compared to previous studies [21], ranging from 0.25 to 0.85, were used to avoid any serious anionic adsorption [18] or mass-transport limitations [5,22], which may arise because of thick Nafion covering layer. Table 1 lists the various physicochemical properties of the solvents used in this

study. Table 2 shows the catalyst ink compositions used to improve the DT process in this work.

2.2. Materials characterization

Field-emission scanning electron micrograph (SEM) analysis was performed with a Jeol JSM-6330F to obtain the microstructure of the surface and cross-section region of MEA. The thickness and degree of contact between membrane and electrode were verified by cross-section SEM analysis. Before characterization, a small square-shaped sample in size of $3 \text{ mm} \times 3 \text{ mm}$ was prepared in the center of the MEA.

2.3. Electrochemical characterization

To examine cell polarization, the prepared MEA was sandwiched in two carbon papers with microporous layers (10BC, SGL, Wiesbaden, GER) and assembled with 9 cm^2 , three-serpentine cell fixture at 70 kgf cm . Ultrapure hydrogen and oxygen gas feed were supplied into the cell at 70°C and ambient pressure, while humidification temperature was maintained at 70°C and 65°C for anode and cathode, respectively. For decal-transferred MEA, an intermediate humidification level in the cathode is better than the fully humidified condition. To obtain stable data, the cell was primarily activated by supplying a gas feed at a fixed flow rate of 120 sccm for 24 h before characterization. During the cell activation, the cell voltage was fixed at 0.5 V or less to avoid serious degradation of the MEA, which is usually observed in high-potential holding condition. During the characterization, the EIS was measured at 0.80 V using a potentiostat/galvanostat working as an impedance analyzer (Gamry Reference 3000, Gamry Instruments, Warmister, PA, USA). The AC amplitude and frequency range were set as 5 mV and from 20,000 Hz–0.1 Hz, respectively. In addition, a constant-current

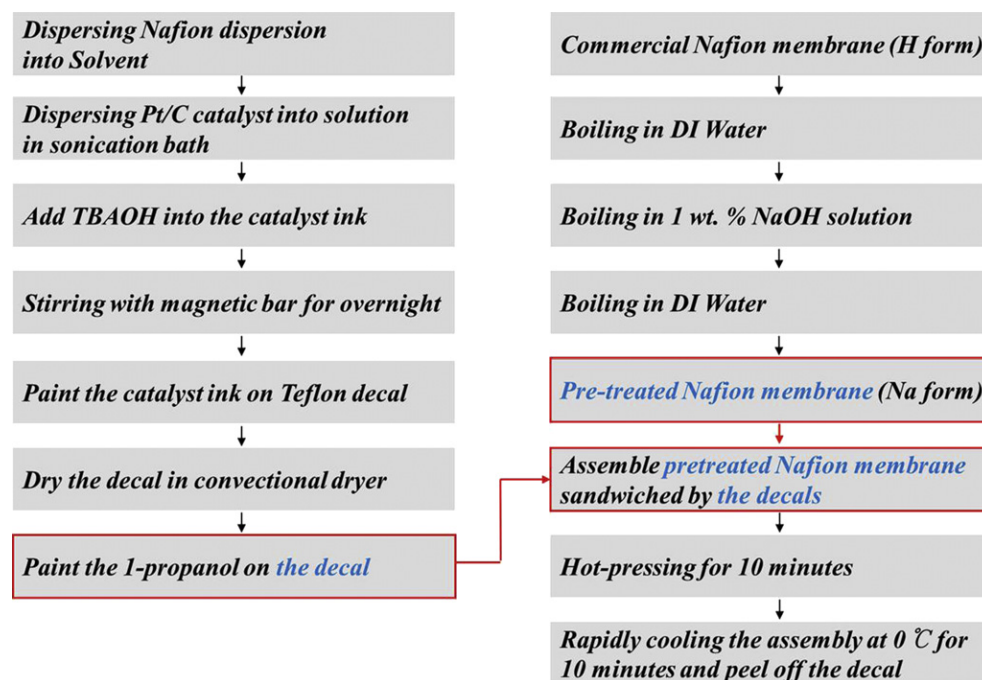
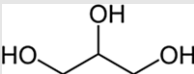
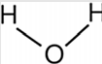



Fig. 2 – A schematic representation of the experimental procedures of the decal-transfer process in this work.

Table 1 – Summary of the physicochemical properties of the solvents, which are generally used to prepare the catalyst ink in the decal-transfer method [25,34,35].

Sample	Chemical structure	Dielectric constant at 328.15 K	Boiling point (K)	Viscosity (cP) at 328.15 K
Glycerol		42.5	563	111.7
Water		60–68	373	1.0
1-Propanol		22.2	370	1.9

load was applied for long-term period to observe cell polarization variations in the aged MEA. During the aging process, applied current of 1.0 A cm^{-2} was maintained for 500 h. At every 100 h, cell polarizations were measured for three times.

For CV analysis, ultrapure hydrogen and nitrogen gas feed were supplied into the cell at 25°C and 20 sccm, while humidification temperature was maintained at 30°C . CV was performed by cycling the potential from 0.05 V to 1.20 V at 50 mV s^{-1} . The amount of charge involved in atomic hydrogen adsorption is used to calculate the electrochemical surface area (ECSA), after influence of double-layer charging/dis-charging and hydrogen evolution reaction are corrected.

3. Results and discussions

3.1. Effect of the glycerol-to-carbon ratio

To clarify the glycerol-to-carbon ratio (GCR) effect on cell performance, MEAs were prepared using DTs with three different GCRs of 6.0, 12.0 and 18.0, which represent low, intermediate and high glycerol content in the catalyst ink. The GCR effect has been mentioned earlier by Chisaka and Daiguji [12]. Although they have clarified the effect of glycerol removal on cell performance, the GCR effect on cell performance after glycerol removal is still unknown. Therefore, we evaluated the

effect of GCR to better understand DT and to estimate the reference GCR value in further sections.

Fig. 3 presents the SEM results for the surface of CLs prepared by the typical CCG method and the DT method. Fig. 3A shows that cracks in the CL are caused by underlying cracks in the GDL with the CCG method, because it is a coating and drying of CL occurs on macroporous carbon paper or cloth with pore sizes ranging from 0.1 to $100 \mu\text{m}$ [23]. Fig. 3B shows that the CL is aggregated at a maximum size of $1 \mu\text{m}$. As seen in the figure, the agglomerated Pt/C and Nafion are not well connected, compared to Fig. 3F. Fig. 3C–F show decal-transferred CLs, which were boiled and converted it into protonated form. The decal transferred CLs with low and high GCR values of 6.0 and 18.0 are presented in Fig. 3C/3D and 3E/3F, respectively. Fig. 3C shows that low-GCR CL surface is filled with cracks as large as $20 \mu\text{m}$. This indicates GCR of 6.0 is insufficient for stable formation of the CLs. Fig. 3D suggests that the agglomerated structure is well connected, however, an average size of the agglomerates was similar to Fig. 3B. Fig. 3E demonstrates that high-GCR CL has no sign of cracks for the $\times 500$ SEM results. In addition, Fig. 3F indicates that high-GCR CL shows that Pt/C being less agglomerated and dense morphology than CCG (Fig. 3B) and low-GCR CL (Fig. 3D).

The graphs in Fig. 4 show the cell polarization and power density curves among three different GCR cases; sample #1–1, #1–2 and #1–3 represents low-, intermediate- and high-glycerol loading cases, obtained by maintaining the GCR as 6.0, 12.0 and 18.0, respectively. As shown in the figure, a remarkable difference in cell polarization is evident between #1–1 and #1–2. The cell polarization of #1–1 shows a performance decrease for both the low-current, activation region and the intermediate-current, ohmic region, relative to #1–2. Recalling the cracks in #1–1 and sharp voltage drop in the activation and ohmic region, it can be deduced that the catalytic activation and proton transfer are greatly hindered by morphological disconnectivity. In addition, a low degree of dispersion, caused by lack of the appropriate amount of solvent, resulted in a more aggregated microstructure, causing a great decrease in the ohmic region. However, there is no noticeable difference in the activation region, between #1–2 and #1–3; a difference in ohmic drop can be observed. The EIS analysis in Fig. 5 indicates that both the anode and

Table 2 – Summary of the solvent-to-carbon ratio and Nafion-to-carbon ratio to fabricate the membrane electrode assembly by the decal transfer.

Sample	Solvent	Solvent-to-carbon ratio	Nafion-to-carbon ratio
#1-1	Glycerol	6.0	0.85
#1-2	Glycerol	12.0	0.85
#1-3	Glycerol	18.0	0.85
#2-1	Glycerol	12.0	0.25
#2-2	Glycerol	12.0	0.45
#2-3	Glycerol	12.0	0.65
#2-4	Glycerol	12.0	0.85

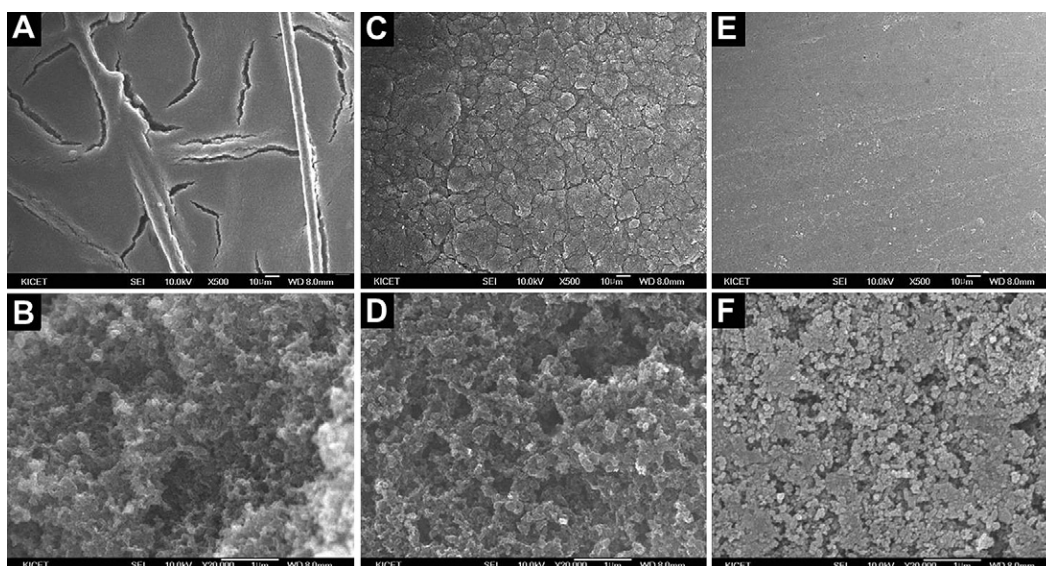


Fig. 3 – SEM images of the surface of the catalyst layer, including A and B: CCG, C and D: decal transfer with low glycerol content (GCR: 6.0) and E, F: decal transfer with high glycerol content (GCR: 18.0), by fixing platinum loading as 0.20 mg cm^{-2} .

cathode charge transfer resistance, $R_{ct,a}$ and $R_{ct,c}$, of #1–3 are similar to #1–2, while high-frequency resistance (HFR) of #1–3 is higher than #1–2. As tabulated in the Table 3, the EIS fit parameters show that charge transfer resistances of #1–3 are even slightly lower than #1–2; the HFR of #1–3 is higher than #1–2, by approximately 0.02 Ohm cm^2 .

The commercial 5 wt.% Nafion dispersion contains 93 wt.% of water and 1-propanol [24], which affects solution properties because the glycerol content is too low. When a sufficient amount of glycerol is present, the properties of the catalyst-ink solution are dominated by the properties of glycerol, hence improving aggregation and cracking in the electrodes because of the high dielectric constant (46.6 [25]), boiling point (280°C) and dispersibility. Therefore, it is reasonable that there are no polarization differences in the activation region, when a sufficient amount of glycerol is present. In addition,

given the EIS result (Fig. 5) and boiling point of glycerol (Table 1), residual amount of glycerol in the CLs might have increased the HFR. Therefore, the evaluation reveals that the amount of glycerol near the threshold GCR value of approximately 12.0 is sufficient, because only the annealing duration increases in proportion to the increase in glycerol content.

3.2. Effect of Nafion-to-carbon ratio

Fig. 6 shows the SEM results of the surface on the CL with different NCRs. The $\times 20,000$ and $\times 100,000$ SEM results of the CL, including NCR of 0.45, 0.65 and 0.85 are presented in Fig. 6A, B and C, respectively. As the NCR increases, the connected region becomes more densely packed because the Nafion binds the Pt/C catalysts into a compact grape-like

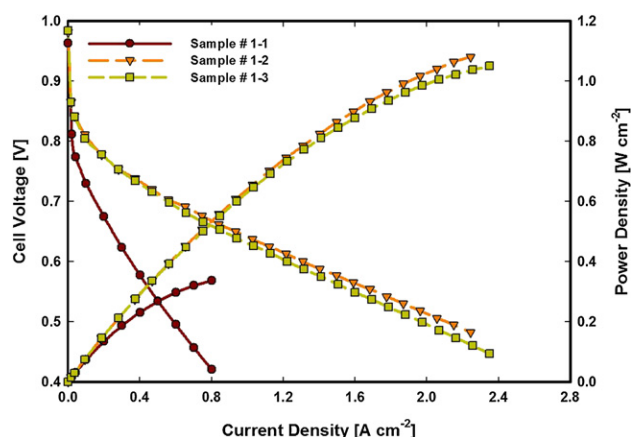


Fig. 4 – Cell polarization and power density curve, including #1-1: glycerol-to-carbon ratio of 6.0, #1-2: glycerol-to-carbon ratio of 12.0 and #1-3: glycerol-to-carbon ratio of 18.0, by fixing Nafion-to-carbon ratio as 0.85.

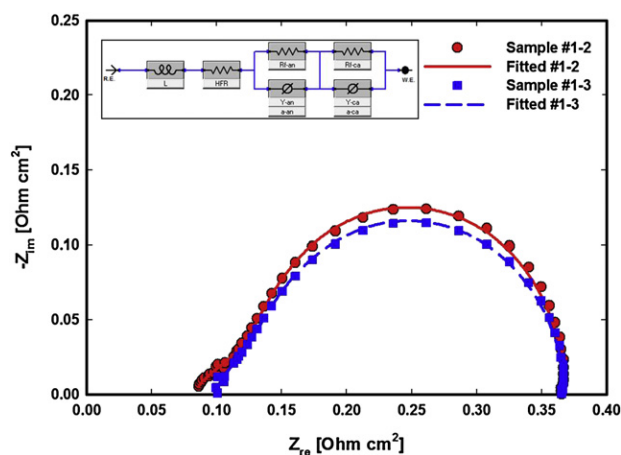


Fig. 5 – Comparison of electrochemical impedance spectroscopy data between #1-2: glycerol-to-carbon ratio of 12.0 and #1-3: glycerol-to-carbon ratio of 18.0, by fixing Nafion-to-carbon ratio as 0.85.

Table 3 – Electrochemical impedance spectroscopy properties of the MEAs prepared from various glycerol-to-carbon ratios.

Sample	HFR ($\Omega \text{ cm}^2$)	$R_{ct,a}$ ($\Omega \text{ cm}^2$)	$R_{ct,c}$ ($\Omega \text{ cm}^2$)	Y_{an}	a_{an}	Y_{ca}	a_{ca}	L (H)
#1-2	0.07954	0.06737	0.24791	0.9007	0.5811	0.1846	0.9670	5.22×10^{-10}
#1-3	0.09377	0.06498	0.22406	0.8289	0.5857	0.1847	0.9865	9.642×10^{-8}

shape. At a magnification of $\times 100,000$, the SEM results suggest that the increased Nafion content has no significant influence on the size of agglomerates in the CL. The agglomerates maintain a similar size, approximately from 100 nm to 200 nm in diameter, although the Nafion content in the CL is triple. As seen in Fig. 6C, abundant Nafion contributed to formation of more dense agglomerate and enhanced connectivity among the agglomerates.

Fig. 7 presents the cross-sectional SEM results on the different MEAs; the MEAs with NCRs of 0.45, 0.65 and 0.85 are shown in Fig. 7A, B and C, respectively. It is known that CL thickness is significantly affected by CL coating [7] or annealing method [26], but not composition. However, in the modified DT, 1-propanol is sufficiently adsorbed in Nafion to reduce softening temperature and hot-pressing pressure. In this work, influence of the NCR on CL thickness differed from that of the conventional DT. On the whole, CL thickness increased and contact was enhanced with increasing NCR. However, as shown in Fig. 7A, a MEA with an insufficient amount of Nafion resulted in poor contact between the membrane and CL. Therefore, it is predicted that polarization difference in the activation region is small due to

morphological resemblance when sufficient amount of NCR is provided.

Fig. 8 show the cell polarization and power density curves among four different NCR cases; sample #2-1, #2-2, #2-3 and #2-4 represents the NCR of 0.25, 0.45, 0.65 and 0.85, respectively. As shown in the figure, a remarkable difference in cell polarization is observed among #2-1 and the other cases. The cell polarization of #2-1 shows a performance decrease for both the low-current, activation region and the intermediate-current, ohmic region, compared to high NCR cases. However, #2-2, #2-3 and #2-4 MEAs presented similar activation polarization. It is noteworthy that #2-3 and #2-4 MEAs showed perfectly overlapped cell polarization on the whole region. By using the modified DT, the CLs with similar electrochemical properties are reproducible when sufficient amount of Nafion is applied. Recalling the microstructures in Fig. 6 and a slight improvement of the ohmic polarization in #2-3, compared to #2-2, it can be deduced that the additional Nafion gave good connectivity among the agglomerates, hence enhancing the effective proton transfer in the CLs. Therefore, the optimum value of NCR can be estimated as 0.65 when whole cell polarization is considered. This value is very low compared to

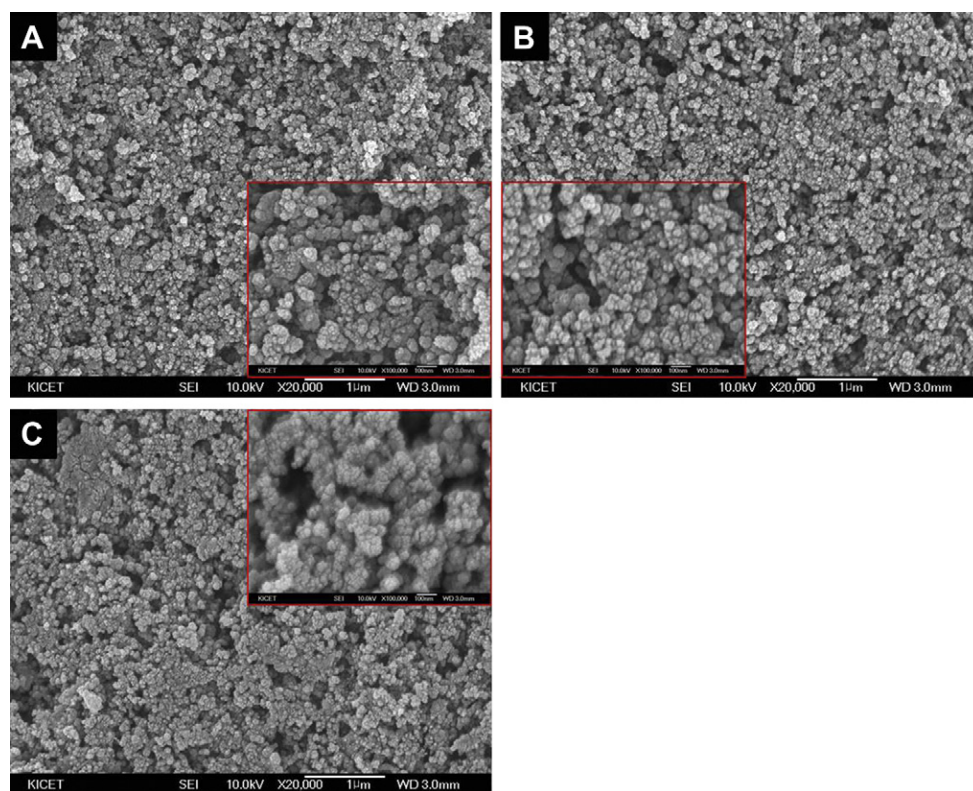


Fig. 6 – SEM images of the surface of the catalyst layer, including A: Nafion-to-carbon ratio of 0.45 (#2-2), B: Nafion-to-carbon ratio of 0.65 (#2-3) and C: Nafion-to-carbon ratio of 0.85 (#2-4), obtained by fixing the glycerol-to-carbon ratio and platinum loading at 12.0 and 0.20 mg cm^{-2} , respectively.

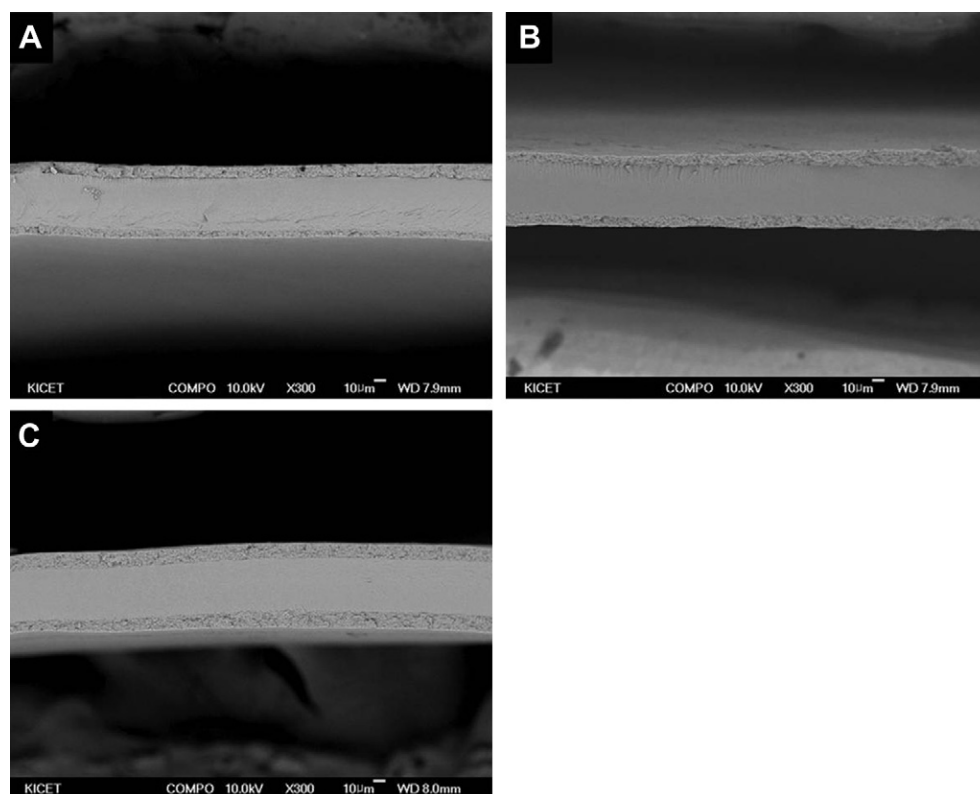


Fig. 7 – SEM images of the cross-sectional surface on the membrane electrode assembly, including A: Nafion-to-carbon ratio of 0.45 (#2-2), B: Nafion-to-carbon ratio of 0.65 (#2-3) and C: Nafion-to-carbon ratio of 0.85 (#2-4), obtained by fixing the glycerol-to-carbon ratio and platinum loading at 12.0 and 0.20 mg cm^{-2} , respectively.

previous literature [27] that has used NCR values as high as 1.5. According to the formation of the agglomerate (Fig. 1), amount of Nafion required should be decreased as size of the agglomerate decreases.

Fig. 9 shows CV results of various NCRs, including 0.25, 0.45, 0.65 and 0.85. As seen in the figure, #2-1, which has the lowest Nafion content, resulted in the lowest ECSA of 25.32 $\text{m}^2 \text{g}^{-1}$, while #2-2 had ECSA of 43.58 $\text{m}^2 \text{g}^{-1}$. Conversely,

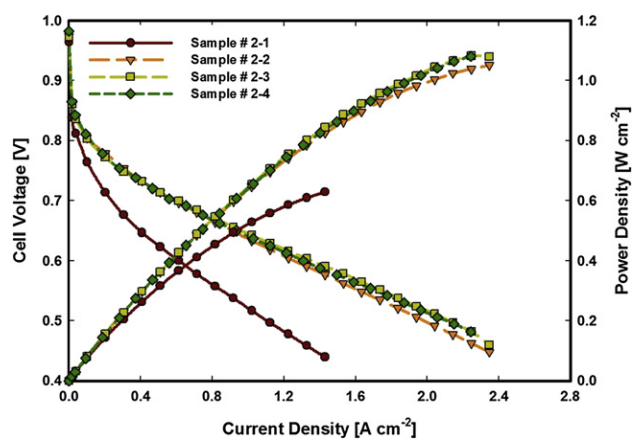


Fig. 8 – Cell polarization and power density curve, including #2-1: Nafion-to-carbon ratio of 0.25, #2-2: Nafion-to-carbon ratio of 0.45, #2-3: Nafion-to-carbon ratio of 0.65 and #2-4: glycerol-to-carbon ratio of 0.85, obtained by fixing the glycerol-to-carbon ratio and platinum loading at 12.0 and 0.20 mg cm^{-2} , respectively.

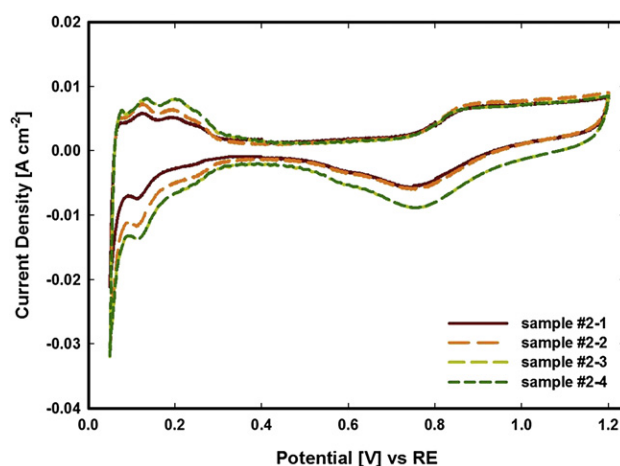


Fig. 9 – Cyclic voltammetry of various MEAs, including #2-1: Nafion-to-carbon ratio of 0.25, #2-2: Nafion-to-carbon ratio of 0.45, #2-3: Nafion-to-carbon ratio of 0.65 and #2-4: glycerol-to-carbon ratio of 0.85, obtained by fixing the glycerol-to-carbon ratio and platinum loading at 12.0 and 0.20 mg cm^{-2} , respectively.

Table 4 – Cyclic voltammetry properties of the MEAs prepared from various Nafion-to-carbon ratios.

Sample	ECSA ^a (m ² g ⁻¹)	i _{dl} ^b (mA cm ⁻²)	C _{dl} ^c (mF cm ⁻²)	A _{Pt} ^d (cm ² cm ⁻²)	Pt utilization ^e (%)
#2-1	25.32	1.17	23.40	50.64	43.53
#2-2	43.58	1.32	26.40	87.16	74.92
#2-3	51.25	1.65	32.94	102.50	88.10
#2-4	50.81	1.67	33.38	101.62	87.35

a Electrochemical surface area obtained from hydrogen adsorption region in cyclic voltammetry results.

b Capacitive current due to charging/discharging of the electrical double layer obtained at 0.4 V.

c Specific capacitance of the electrical double layer, $C_{dl}(\text{F cm}^{-2}_{\text{MEA}}) = i_{dl}/\text{potential sweeping rate}(= 50 \text{ mVs}^{-1})$.

d Specific area of the platinum catalysts, $A_{Pt}(\text{cm}^2_{\text{Pt}} \text{ cm}^{-2}_{\text{MEA}}) = \text{ECSA} \times \text{Platinum Loading}(= 0.20 \text{ mg cm}^{-2})$.

e Platinum utilization, Pt utilization = $\text{ECSA}/58.17 \text{ m}^2 \text{ g}^{-1}$.

f ECSA of Pt in liquid electrolyte, measured by cyclic voltammetry of commercial Pt/C in 0.5 M H₂SO₄ at 25 °C.

high NCR cases, including #2-3 and #2-4, had the largest and second largest ECSAs of 51.25 m² g⁻¹ and 50.81 m² g⁻¹, respectively. This indicated that the minimum required amount of NCR, which covers or penetrates into the agglomerates in present catalyst-ink solution came between 0.45 and 0.65. Above the thresholding NCR, ECSA remained between 50 m² g⁻¹ and 52 m² g⁻¹, although amount of Nafion content was increased. Therefore, the resulting ECSA of 51.25 m² g⁻¹ from #2-3 can be regarded as optimum value. In addition, platinum utilization was calculated as the ratio of the ECSA of MEA to that of 20 wt.% Pt/C (58.17 m² g⁻¹) measured using CV in liquid electrolyte [28], i.e. 0.5 M H₂SO₄ solution in this paper. The platinum utilization of 88.10% was obtained for #2-3, which exceeds that of conventional DT MEAs, approximately ~80% [29]. The electrochemical properties from CV of various-NCR MEAs are tabulated in Table 4.

Fig. 10 shows long-term cell polarizations of #2-3, which was obtained under a constant-current load of 1.0 A cm⁻². As seen in the figure, relatively small voltage losses in OCP and

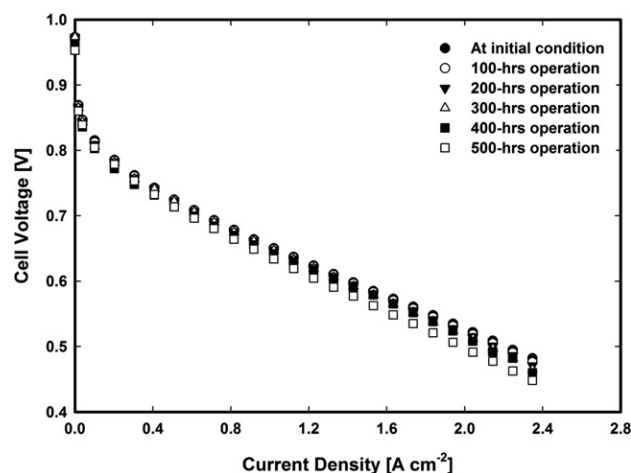


Fig. 10 – Cell polarization curve of #2-3 during 500-h operation.

low-current polarization were obtained as ~20 mV, which is lower than the previous literature [30]. According to recent carbon-oxidation simulation results [31,32], a small voltage loss of ~20 mV for 500-h case in low-current polarization indicates that the rate of carbon-oxidation reaction is relatively mild at present constant-current condition. For intermediate- and high-current polarization, the ionomer-aging effect resulted in similar degree of voltage loss, which is approximately 50 mV at 2.0 A cm⁻². By considering molecular-dynamics simulation result from Malek and Franco [17], the low-current polarization data suggests that low NCR MEA may prevent early transition of Nafion-CB surfaces from hydrophobic to hydrophilic state, which directly accelerate carbon-support oxidation. Because transient variations in CL microstructures are dependent on carbon-support selection [33], further studies are recommended to examine carbon-corrosion durability of the low-NCR MEAs by employing graphitized-carbon supports.

4. Conclusions

In this paper, the effects of GCR and NCR in decal-transferred MEAs on a single cell performance were evaluated. Using the DT, the resulting MEAs were characterized by SEM, direct-current cell polarization, CV and EIS at a fixed platinum loading of approximately 0.20 mg cm⁻². The following conclusions could be drawn from this study:

- i) The effect of GCR on cell performance was examined by preparing MEAs with low, intermediate and high glycerol-containing catalyst ink with GCRs of 6.0, 12.0 and 18.0, respectively. When low glycerol-containing catalyst ink was used, solvent properties of the ink were dominated by the properties of DI water and 1-propanol because 5 wt.% Nafion dispersion was employed. In addition, a series of cracks were observed in a low micrometer scale, due to easy evaporation of the solvent. For this reason, the low glycerol MEA gave a much poorer cell performance than the other MEAs. Meanwhile, the intermediate and high glycerol MEAs showed similar cell performance because the catalyst ink is dominated by glycerol properties. The evaporation rate was sufficiently slow and no crack was observed due to the relatively high boiling point of glycerol, 280 °C.
- ii) The effect of NCR on cell performance was examined by preparing various catalyst inks with four different Nafion contents of 0.25, 0.45, 0.65 and 0.85. The lowest NCR MEA was shown to have a lower cell performance than the other MEAs. From CV analysis, an insufficient amount of Nafion content resulted in great decline of the ECSA. Conversely, the high NCR MEAs, including NCRs of 0.65 and 0.85, resulted in similar ECSAs because a sufficient amount of Nafion to construct the agglomerates was added to the resulting CLs. They presented the most improved cell polarizations, which are surprisingly similar in whole region. Because sufficient amount of Nafion was evident in the NCR of 0.65 to cover and connect the agglomerates in the CL, it can be concluded that the optimized NCR is 0.65.

Acknowledgements

This work was supported by the Manpower Development Program for Energy supported by the Ministry of Knowledge and Economy (MKE). This work was also partially supported by the Mid-career Researcher Program through the National Research Foundation of Korea (NRF) funded by the Ministry of Education, Science and Technology (2011-0029249). The authors are grateful for their financial support.

REFERENCES

- [1] Marcinkoski J, Kopasz JP, Benjamin TG. Progress in the US DOE fuel cell subprogram efforts in polymer electrolyte fuel cells. *Int J Hydrogen Energy* 2008;33:3894–902.
- [2] Johnson Matthey Plc. Platinum 2011; 2011, p. 25–35.
- [3] Zhu W, Ku D, Zheng JP, Liang Z, Wang B, Zhang C, et al. Buckypaper-based catalytic electrodes for improving platinum utilization and PEMFC's performance. *Electrochim Acta* 2010;55:2555–60.
- [4] Shah AA, Kim GS, Gervais W, Young A, Promislow K, Li J, et al. The effects of water and microstructure on the performance of polymer electrolyte fuel cells. *J Power Sources* 2006;160:1251–68.
- [5] Jung CY, Park CH, Lee YM, Kim WJ, Yi SC. Numerical analysis of catalyst agglomerates and liquid water transport in proton exchange membrane fuel cells. *Int J Hydrogen Energy* 2010;35:8433–45.
- [6] Ticianelli EA, Derouin CR, Redondo A, Srinivasan S. Methods to advance technology of proton exchange membrane fuel cells. *J Electrochem Soc* 1988;135:2209–14.
- [7] Wilson MS, Gottesfeld S. High performance catalyzed membranes of ultra-low Pt loadings for polymer electrolyte fuel cells. *J Electrochem Soc* 1992;139:L28–30.
- [8] Wilson MS, Gottesfeld S. Thin-film catalyst layers for fuel cell electrodes. *J Appl Electrochem* 1992;22:1–7.
- [9] Wilson MS, Valerio JA, Gottesfeld S. Low platinum loading electrodes for polymer electrolyte fuel cells fabricated using thermoplastic ionomers. *Electrochim Acta* 1995;40:355–63.
- [10] Xie J, More KL, Zawodzinski TA, Smith WH. Porosimetry of MEAs made by “thin film decal” method and its effect on performance of PEFCs. *J Electrochem Soc* 2004;151:A1841–6.
- [11] Xie J, Garzon F, Zawodzinski T, Smith W. Ionomer segregation in composite MEAs and its effect on polymer electrolyte fuel cell performance. *J Electrochem Soc* 2004;151:A1084–93.
- [12] Chisaka M, Daiguji H. Effect of glycerol on micro/nano structures of catalyst layers in polymer electrolyte membrane fuel cells. *Electrochim Acta* 2006;51:4828–33.
- [13] Saha MS, Paul DK, Peppley BA, Karan K. Fabrication of catalyst-coated membrane by modified decal transfer technique. *Electrochem Commun* 2010;12:410–3.
- [14] Cho JH, Kim JM, Prabhuram J, Hwang SY, Ahn DJ, Ha HY, et al. Fabrication and evaluation of membrane electrode assemblies by low-temperature decal methods for direct methanol fuel cells. *J Power Sources* 2009;187:378–86.
- [15] Park HS, Cho YH, Cho YH, Park IS, Jung N, Ahn M, et al. Modified decal method and its related study of microporous layer in PEM fuel cells. *J Electrochem Soc* 2008;155:B455–60.
- [16] Cho HJ, Jang H, Lim S, Cho EA, Lim TH, Oh IH, et al. Development of a novel decal transfer process for fabrication of high-performance and reliable membrane electrode assemblies for PEMFCs. *Int J Hydrogen Energy* 2011;36:12465–73.
- [17] Malek K, Franco AA. Microstructure-based modeling of aging mechanisms in catalyst layers of polymer electrolyte fuel cells. *J Phys Chem B* 2011;115:8088–101.
- [18] Subbaraman R, Strmcnik D, Stamenkovic V, Markovic NM. Three phase interfaces at electrified metal-solid systems 1. Study of the Pt(hkl)-Nafion interface. *J Phys Chem C* 2010;114:8414–22.
- [19] Bender G, Zawodzinski TA, Saab AP. Fabrication of high precision PEFC membrane electrode assemblies. *J Power Sources* 2003;124:114–7.
- [20] Kim YS, Lee KS, Rockward T, US Patent; 2010, 20100183804.
- [21] Suzuki T, Tsushima S, Hirai S. Effect of Nafion® ionomer and carbon particles on structure formation in a proton-exchange membrane fuel cell catalyst layer fabricated by the decal-transfer method. *Int J Hydrogen Energy* 2011;36:12361–9.
- [22] Kamarajugadda S, Mazumder S. Numerical investigation of the effect of cathode catalyst layer structure and composition on polymer electrolyte membrane fuel cell performance. *J Power Sources* 2008;183:629–42.
- [23] Chun JH, Park KT, Jo DH, Lee JY, Kim SG, Lee ES, et al. Determination of the pore size distribution of micro porous layer in PEMFC using pore forming agents under various drying conditions. *Int J Hydrogen Energy* 2010;35:11148–53.
- [24] DuPont™ Fuel Cells. Product information—DuPont™ Nafion® PFSA polymer dispersions. Delaware: DuPont™; 2009.
- [25] Uchida M, Aoyama Y, Eda N, Ohta A. New preparation method for polymer-electrolyte fuel cells. *J Electrochem Soc* 1995;142:463–8.
- [26] Yoon YJ, Kim TH, Kim SU, Yu DM, Hong YT. Low temperature decal transfer method for hydrocarbon membrane based membrane electrode assemblies in polymer electrolyte membrane fuel cells. *J Power Sources* 2011;196:9800–9.
- [27] Janssen GJM, Sitters EF. Performance of thin-film cathodes for proton-exchange-membrane fuel cells based on high-surface-area carbon supports. *Power Sources* 2007;171:8–17.
- [28] Saha MS, Malevich D, Halliop E, Pharoah JG, Peppley BA, Karan K. Electrochemical activity and catalyst utilization of low Pt and thickness controlled membrane electrode assemblies. *J Electrochem Soc* 2011;158:B562–7.
- [29] Carter RN, Kocha SS, Wagner FT, Fay M, Gasteiger HA. Artifacts in measuring electrode catalyst area of fuel cells through cyclic voltammetry. *ECS Trans* 2007;11:403–10.
- [30] Liu D, Case S. Durability study of proton exchange membrane fuel cells under dynamic testing conditions with cyclic current profile. *J Power Sources* 2006;162:521–31.
- [31] Franco AA, Gerard M. Multiscale model of carbon corrosion in a PEFC: coupling with electrocatalysis and impact on performance degradation. *J Electrochem Soc* 2008;155:B367–84.
- [32] Jung CY, Kim WJ, Yi SC. Computational analysis of mixed potential effect in proton exchange membrane fuel cells. *Int J Hydrogen Energy* 2012;37:7654–68.
- [33] Malek K, Mashio T, Eikerling M. Microstructure of catalyst layers in PEM fuel cells redefined: a computational approach. *Electrocatalysis* 2011;2:141–57.
- [34] Segur JB, Oberstar HE. Viscosity of glycerol and its aqueous solutions. *Ind Eng Chem* 1951;43:2117–20.
- [35] Aldrich Chemistry. 2012–2014 Handbook of fine chemistry. Sigma Aldrich.